NASA TECHNICAL NOTE

NASA TN D-5231

C. 1

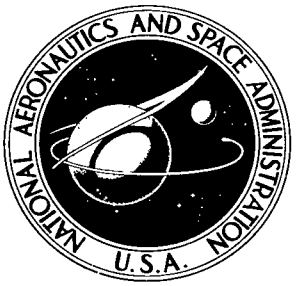

NASA TN D-5231

DETERMINATION OF LUNAR EQUATORIAL RADIUS USING IMAGE-MOTION COMPENSATION SENSOR DATA FROM LUNAR ORBITER I

by Harold R. Compton and William R. Wells

Langley Research Center
Langley Station, Hampton, Va.

NATIONAL AERONAUTICS AND SPACE ADMINISTRATION • WASHINGTON, D. C. • JUNE 1969

DETERMINATION OF LUNAR EQUATORIAL RADIUS USING IMAGE-MOTION COMPENSATION SENSOR DATA FROM LUNAR ORBITER I

By Harold R. Compton and William R. Wells

Langley Research Center
Langley Station, Hampton, Va.

NATIONAL AERONAUTICS AND SPACE ADMINISTRATION

For sale by the Clearinghouse for Federal Scientific and Technical Information
Springfield, Virginia 22151 – CFSTI price $3.00

DETERMINATION OF LUNAR EQUATORIAL RADIUS USING IMAGE-MOTION COMPENSATION SENSOR DATA FROM LUNAR ORBITER I

By Harold R. Compton and William R. Wells
Langley Research Center

SUMMARY

The telemetry data from the image-motion compensation sensor (V/H sensor) on the Lunar Orbiter I spacecraft have been analyzed to determine the radius of the moon in the equatorial region from about 50° west to about 40° east selenographic longitude. The results of this report indicate that over this region, the lunar radii determined from these data vary from a minimum of 1734.6 km to a maximum of 1738.6 km. The arithmetic mean of these radii is 1736.5 km or about 1.5 km smaller than the mission planning value of 1738.09 km prior to the Ranger and Lunar Orbiter series of spacecraft. An asymmetrical bulge toward the earth was noted in the general area of Sinus Medii.

The values of the lunar radii presented in this paper have been compared with those determined from a harmonic analysis, Ranger VIII impact analysis, radar measurements, and photogrammetric techniques. Except for the harmonic analysis, these radii are in good agreement with the Lunar Orbiter values.

INTRODUCTION

The Lunar Orbiter I spacecraft was used to photograph various sites in the equatorial region ($\pm 4^{\circ}$ latitude) of the moon. In order to reduce smearing of the photographs due to the motion of the spacecraft with respect to the lunar surface, an electro-optical device known as the image-motion compensation sensor and referred to as the V/H sensor was used. One of the outputs of this sensor was a mechanical shaft rotation proportional to image motion which drove the camera platen through a cam and lever arrangement in such a way as to eliminate image motion. This output was converted to an equivalent linear speed, which was divided by the focal length of the camera lens and this ratio was telemetered back to earth as a V/H measurement. This V/H measurement along with a knowledge of the spacecraft state vector at the time of the measurement is used in this report to determine the radius with respect to the center of mass of the moon at the point of measurement.

Before calculations of the lunar radii could be made, it was necessary to determine the position and velocity, spacecraft state vector, of the Lunar Orbiter I spacecraft at that time associated with each V/H readout. This determination was made by using a special-purpose orbit-determination computer program which made use of the procedures of iterative differential corrections, weighted least squares, and numerical integration of the equations of motion of the lunar spacecraft. The spacecraft states were used in conjunction with the V/H data to determine the lunar radius at various points in the equatorial region of the moon.

A determination of the lunar radius by using the V/H measurement offers a distinct advantage over certain previous determinations such as those from earth-based radar instruments. Determinations using earth-based radar preclude a knowledge of the earth-moon distance which enters directly into the calculations of the lunar radii. However, for determination of lunar radii using the V/H data, the earth-moon distance enters indirectly into the calculations and hence is not a prominent error source.

SYMBOLS

e	eccentricity of lunar satellite orbit
f	focal length
H	distance from P_1 to P_4 (see fig. 2)
H_1, H_2	local horizontals at points P_1 and P_2, respectively (see fig. 2)
i	inclination of lunar satellite plane to the lunar equatorial plane
P_1	position of spacecraft at time of orientation of optical axis along local vertical of photo site
P_2	position of spacecraft at photo time
P_3	point on lunar surface which is scanned by V/H sensor
P_4	point of intersection of a line drawn from P_3 perpendicular to optical axis
r	magnitude of spacecraft radius vector from center of mass of moon
$\bar{r}$	spacecraft radius vector from center of mass of moon

R	magnitude of lunar radius
v	true anomaly of spacecraft
V	component of spacecraft velocity normal to optical axis
V_p	camera platen speed
V_s	spacecraft speed
X,Y,Z	selenographic Cartesian coordinate system
β	angle measured between spacecraft radius vector $\bar{r}$ and lunar radius vector to point being scanned
η	angle measured between local vertical and optical axis
γ	flight-path angle measured between spacecraft velocity vector and local horizontal
λ	selenographic longitude (see fig. 3)
Ω	longitude, measured from positive X-axis, of ascending node of lunar satellite orbit (see fig. 3)
ω	argument of periapse
φ	selenographic latitude (see fig. 3)
θ	angle measured between lines P_1P_4 and P_1P_3 (see fig. 2)

ANALYSIS

Operation of V/H Sensor

The V/H sensor is located on the Lunar Orbiter spacecraft so that it scans the lunar surface through a portion of the 24-inch (0.6096 meter) camera lens which is outside the normal image format. A small rectangular aperture, 0.125 inch by 0.035 inch (3.175 mm by 0.89 mm), is located on a scanner disk and rotates in a circle at the rate of 4000 rpm or one scan every 0.015 second. The distance from the center of rotation to the center

of the aperture is 0.6875 inch (17.46 mm). During one scan or one rotation of the rectangular aperture, an annulus which has an outer radius of approximately 1.6 km and an inner radius of about 1.3 km is swept out on the surface of the moon. Between successive rotations of the scanner disk, the lunar scene necessarily changes because of the motion of the spacecraft. The V/H sensor detects the shift in the image and attempts to reduce or null the image shift by changing the camera-platen speed. (See fig. 1 which was taken from ref. 1.)

In order to detect the change in the lunar scene, the rectangular aperture transmits light rays from the camera-lens image plane to a photomultiplier tube through a series of mirrors which are attached to the disk. The photomultiplier tube senses variations in the lunar surface brightness within the annulus and hence produces a time-varying electrical output. This electrical output is used to determine the light intensity. If the light intensity is above a predetermined level, an electrical signal is fed into the electronic circuitry which then produces a change in the speed of the camera platen. If the light is below the predetermined level, the camera platen continues to run at the original speed. A more detailed description of the V/H sensor and its operation is given in reference 1.

It is convenient to speak of the V/H tracking cycle. This tracking cycle is defined by the motion of the tracking optics over a fixed interval during which time the V/H axis to the lunar surface varies from about 10° to 6° ahead of the camera optical axis from start to finish of the tracking cycle. However, the exact angle between the V/H axis and optical axis at any given time is not known. For the purpose of this analysis, it was assumed that on the average, this angle is 8°. At the end of each tracking cycle, the V/H axis was reset to a position 10° ahead of the optical axis and a new tracking cycle was begun.

In general, operation of the V/H sensor was initiated just prior to photographing a given site. The selenographic latitude and longitude of the desired photo site were predetermined and shortly before a picture-taking sequence the camera optical axis was alined along a direction parallel to the local vertical of the desired photo site. The V/H sensor was then put into operation and used to control the camera platen speed throughout the photographing sequence. The V/H sensor continued to operate for a short time after termination of photography. Hence, V/H telemetry was available from a time just prior to and until a time just shortly after photographing of each site. Usually the V/H readouts were available at 23-second intervals over this period of time.

Analytical Expression for Lunar Radius

As stated earlier, one of the V/H outputs was a mechanical shaft rotation proportional to image motion which drove the camera platens through a cam and lever arrangement in such a way as to eliminate image motion. In particular, this output was converted

to an equivalent linear speed which was then divided by the focal length of the camera. The result was the V/H reading and it is equal to the ratio of the spacecraft speed (normal to the optical axis) to the object distance.

Before presenting the equation for the lunar radius, it is appropriate to illustrate the spacecraft—lunar-surface geometry. (See fig. 2.) The position of the spacecraft at the time of orientation of the optical axis along the local vertical of the photo site is shown as P_1 where the local vertical to the photo site is the line from P_2 to the center of the moon. The line P_1P_3 is along the V/H axis and P_3 is the point on the lunar surface which is being scanned by the V/H sensor. The line P_1P_4 is parallel to the optical axis and its length is equivalent to the object distance. The local horizontals at P_1 and P_2 are parallel to H_1 and H_2, respectively. The angle between the V/H axis and the optical axis of the 24-inch (0.6096-meter) lens is θ which is assumed to have an average value of 8^o. The angle η is called the tilt angle and is the angle between the local vertical and the optical axis at any given time. The time history of this angle was obtained from photo support data. (See ref. 2.)

It was stated previously that the V/H reading was equivalent to the ratio of the spacecraft speed (normal to the optical axis) to the object distance. This statement can be written as:

$$\frac{V}{H} = \frac{V_S \cos(\gamma - \eta)}{P_1P_4} \tag{1}$$

where V_S is the spacecraft speed obtained from the orbit determination program. The flight-path angle γ is defined by

$$\tan \gamma = \frac{e \sin v}{1 + e \cos v} \tag{2}$$

and is also obtained from the orbit determination program where v is the true anomaly and e is the eccentricity. The remaining parameters in equation (1) have been previously defined. The angle η is taken to be negative when the optical axis lags the local vertical as in figure 2 and positive when it is ahead of the local vertical.

The equation for the lunar radius is determined from the triangle defined by P_1P_3 and the center of the moon in figure 2. From this triangle

$$R^2 = r^2 + \left(P_1P_3\right)^2 - 2rP_1P_3 \cos(\theta + \eta) \tag{3}$$

where the magnitude of the lunar radius is R and the magnitude of the spacecraft position vector is r and is obtained from the orbit determination program. The quantity P_1P_3 is determined from equation (1) by setting

$$P_1P_4 = P_1P_3 \cos \theta \tag{4}$$

Hence from equations (1) and (4)

$$P_1P_3 = \frac{V_S \cos(\gamma - \eta)}{\frac{V}{H} \cos \theta} \tag{5}$$

Therefore

$$R = \left\{ r^2 + \left[\frac{V_S \cos(\gamma - \eta)}{\frac{V}{H} \cos \theta} \right] \left[\frac{V_S \cos(\gamma - \eta)}{\frac{V}{H} \cos \theta} - 2r \cos(\theta + \eta) \right] \right\}^{1/2} \tag{6}$$

It should be noted that, in general, equation (4) is not exact and in fact by writing this equation a tacit assumption of a flat lunar surface has been made. This assumption is valid for the values of θ and altitude used in this report.

Analytical Expression for Selenographic Latitude and Longitude of Lunar Radius

Equation (6) was used to calculate the lunar radius; however, it is also necessary to calculate the selenographic latitude and longitude of the point of determination of the lunar radius. From figure 3 it can be seen that

$$\left.\begin{aligned} \sin \varphi &= \sin i \sin(\omega + v + \beta) \\ \sin \lambda \cos \varphi &= \cos(\omega + v + \beta)\sin \Omega + \cos i \cos \Omega \sin(\omega + v + \beta) \\ \cos \lambda \cos \varphi &= \cos(\omega + v + \beta)\cos \Omega - \cos i \sin \Omega \sin(\omega + v + \beta) \end{aligned}\right\} \tag{7}$$

where φ is the selenographic latitude and λ is the selenographic longitude. The angles i and ω are the inclination of the lunar satellite orbital plane and the argument of periapse, respectively, and β is the angle between the satellite radius vector and lunar radius being calculated. The angle β can be calculated from the equation

$$\cos \beta = \frac{R^2 - (P_1P_3)^2 + r^2}{2Rr} \qquad (0^\circ < \beta < 90^\circ) \tag{8}$$

RESULTS AND DISCUSSION

The primary results presented in this paper are the lunar radii with respect to the center of mass at 73 points in the equatorial region of the moon. These radii along with the selenographic latitude and longitude of the points of determination are listed in table I

in time-ordered sets according to the time at which V/H telemetry was available. These radii are also plotted in figure 4 as a function of longitude. The maximum latitude for either of these radii is 2.2° north and 4.0° south. The maximum lunar radius is 1738.6 km and occurs in the mountainous region just to the east of the Central Bay (Sinus Medii) area whereas the minimum lunar radius is 1734.6 km and occurs in Mare Tranquillitatis. The arithmetic mean of the 73 values of lunar radii is 1736.5 km or about 1.5 km smaller than the mission planning value of 1738.09 km prior to the Ranger and Lunar Orbiter series of spacecraft. On scanning figure 4 from 50° west to 40° east longitude, there appears to be an asymmetrical bulge toward the earth in the Central Bay area of the lunar equator. This same type of bulge was observed in the results in reference 3.

It is of interest to compare the lunar radii in this paper with those obtained from other techniques. Two such comparisons are given in figure 5. The solid curve in figure 5 represents the results for lunar radius variations in the equatorial region from a harmonic analysis by Bray and Goudas of a selenodetic control system of the U.S. Air Force Aeronautical Chart and Information Center (ACIC) (ref. 4). The radii presented in this curve were derived from earth-based photography and thus are considered to be with respect to the center of figure of the moon. The Lunar Orbiter values are smaller on the average by about 2 km, best agreement being in the region from 30° to 40° east longitude. However, there appears to be a general agreement in the variation of the radius and one can also note an asymmetrical bulge in the solid curve similar to that which was previously pointed out in the Lunar Orbiter values. Also shown in figure 5 is a radius determination with respect to the center of mass of the moon from Ranger VIII impact analysis. (See ref. 5.) This value is in agreement with Lunar Orbiter values. The trends illustrated in figure 5 indicate that the radii relative to the center of mass of the moon are systematically less than those relative to the center of figure. Hence these results may indicate a displacement of the center of mass of the moon toward the earth, relative to the center of figure.

A point-by-point comparison of Lunar Orbiter values with recent radar and photogrammetric determinations is presented in table II. The radar values were taken from reference 3 and were chosen to coincide as closely as possible to the latitude and longitude of the Lunar Orbiter points. The few radar points which are compared are in agreement and appear to support the Lunar Orbiter data. In the lower part of table II, the Lunar Orbiter values are compared point by point with those obtained by using photogrammetric techniques. (See ref. 6.) Note that the latitude and longitude are the same for both sets of radii. The photogrammetric data are lower than the Lunar Orbiter data, differences ranging from 0.2 km to about 0.6 km. Thus, the photogrammetric results are also in agreement with and appear to support the Lunar Orbiter values. Note that

the differences between the Lunar Orbiter values and the radar and photogrammetric values lie well within the respective accuracies of the values presented.

Since the 73 values of the lunar radii were all in the equatorial region of the moon, it seemed of interest to fit the various sets of lunar radii presented in table I to an ellipse which might represent the lunar equator. The lunar equatorial plane was assumed to be elliptical, the major axis being in the direction of Sinus Medii. The sets of radii were combined in various ways and then fitted in a least-squares process to obtain several ellipses. The combination of sets of radii were chosen to obtain ellipses for all data, for all data having west longitude, for all data having east longitude, for all data in smooth areas, and for all data in mountainous areas. The semiaxes and eccentricity of these ellipses are shown in table III. Also shown in table III is an estimate of the mean lunar radius for each ellipse. This estimate was obtained by integrating the radius function over each ellipse and then dividing by the interval of integration. The largest value of the mean radius was obtained from ellipse 1 where the radii were mostly in the rough mountainous region just south of Mare Tranquillitatis from about 30° to 40° east longitude. Ellipse 2 had the largest semimajor axis and eccentricity. The radii in this ellipse were also calculated from mostly mountainous areas. Ellipses 3 and 4 were determined from all data having east and west longitudes, respectively, and it can be seen that the mean radius for each differs by approximately 0.5 kilometer. Ellipse 5 was determined from radii obtained from mostly smooth areas whereas ellipse 6 is a combination of all 73 radii. In general, ellipse 6 is expected to be the most representative of the lunar equator since it contains the largest sample. However, the mean lunar radius is not vastly different for either of the ellipses but differs from the arithmetic mean by about 0.8 kilometer. This difference may be due to the fact that the radii were integrated over the interval from the western limb to the eastern limb whereas the actual radii were all contained in the interval from 50° west to 40° east and hence the mean lunar radius presented in table III is an extrapolated value. However, it is important to note that all calculated values of the mean lunar radius presented in this paper are from 1.5 to 2.5 km less than the value accepted prior to Ranger VII and the Lunar Orbiter flights. Therefore, it might be expected that a mean lunar radius calculated from a larger sample of radii over the entire interval from western limb to eastern limb would be significantly lower than the previously accepted value.

In order to obtain an estimate of possible error associated with the magnitude of the radii, three error sources were considered. They were the uncertainty in the determination of the spacecraft radius, the uncertainty in the angle θ, and the biases associated with the V/H sensor. At this time the V/H biases, if any existed, are not known; however, the sensor was designed to operate between 8 and 50 milliradians per second

and in fact it operated well within this design during the Lunar Orbiter I flight. Also, there has been no evidence from the lunar photographs to indicate that the sensor operated improperly. Therefore, for the purpose of this paper, it was assumed that there was no improper operation or bias of the V/H sensor. The maximum uncertainty in θ and the spacecraft radius has been estimated to be $\pm 2^{o}$ and ± 0.5 km, respectively. By assuming the maximum uncertainty in these two parameters, and assuming that the spacecraft radius error is entirely along the lunar radius, the estimated possible error in the magnitude of the lunar radius is ± 0.7 kilometer.

The locations, selenographic latitudes and longitudes, of the lunar radii have errors associated with them because of the uncertainty in the angle θ, the uncertainty of the V/H sample point within the scanning annulus, and the uncertainty in the orientation of the spacecraft radius vector. The maximum error in the angle θ was assumed to be 2^{o} and this assumption leads to a possible error of 1.7 km in the location of P_3 on the lunar surface. The V/H sample was assumed to have been at the center of the scanning annulus whereas it was somewhere between the outer and inner circle. This assumption leads to a possible error of 1.6 km in the location of P_3 on the lunar surface. Finally, the orientation of the spacecraft radius vector was assumed to be in error by 0.095^{o} of arc at the center of the moon. This assumption corresponds to about a 3-km error at the spacecraft in the position vector and to a possible error of 2.7 km in the location of P_3. By adding the three errors in the location of P_3, a possible error of 6 km or 0.2^{o} central angle is obtained.

CONCLUDING REMARKS

The lunar radius has been determined at 73 points in the equatorial region from about 50^{o} west to 40^{o} east selenographic longitude. The mean lunar radius was found to be from 1.5 to 2.5 km smaller than the accepted value prior to the Ranger VIII and the Lunar Orbiter flights. An asymmetrical bulge toward the earth was noted in the general area of Sinus Medii. Comparisons of the Lunar Orbiter values of the radii were made with those determined from a harmonic analysis, Ranger VIII impact analysis, radar measurements, and photogrammetric technique. In general, the Lunar Orbiter values were in agreement with these data except for those associated with the harmonic analysis and even in this case the variation in the radius agreed very well. It should be noted that the radii presented in this report all lie within a band $\pm 4^{o}$ of the lunar equator and that no limb data has been included. Therefore, in order to substantiate the lower mean value presented in this report, it will be necessary to include data over the entire interval from the western to the eastern limb. It should also be noted that because the radii presented

in this report are with reference to the center of mass of the moon, and not with respect to the center of figure, they may indicate a displacement of the center of mass of the moon toward the earth, relative to the center of figure.

Langley Research Center,
National Aeronautics and Space Administration,
Langley Station, Hampton, Va., April 1, 1969,
185-42-31-02-23.

REFERENCES

1. Anon.: Photographic Subsystem Reference Handbook for the Lunar Orbiter Program. L-018375-RU., Eastman Kodak Co., Mar. 15, 1966.

2. Boeing Co.: Lunar Orbiter I – Postmission Photo Supporting Data. NASA CR-66481, 1967.

3. Shapiro, A.; Uliana, E. A.; Yaplee, B. S.; and Knowles, S. H.: Lunar Radius From Radar Measurements. Cospar Moon and Planets II, A. Dollfus, ed., North-Holland Publ. Co., c.1968, pp. 34-46.

4. Bray, T. A.; and Goudas, C. L.: A Contour Map Based on the Selenodetic Control System of A.C.I.C. Icarus, vol. 5, no. 5, 1966, pp. 526-535.

5. Sjogren, William J.; Trask, Donald W.; Vegos, Charles J.; and Wollenhaupt, Wilbur R.: Physical Constants as Determined From Radio Tracking of the Ranger Lunar Probes. Space Flight Mechanics Specialist Symposium, Vol. 11, Maurice L. Anthony, ed., Amer. Astronaut. Soc., 1967, pp. 137-154.

6. Jones, Ruben L.: An Analytical Study of Lunar Surface Shape and Size From Lunar Orbiter Mission I Photographs. NASA TN D-5243, 1969.

TABLE I.- RADII IN EQUATORIAL REGION OF MOON

Radii, km	Latitude, deg	Longitude, deg
	Set I	
1737.83	1.75	29.58
1736.84	1.48	30.89
1736.51	1.20	32.21
1737.83	.92	33.53
1736.97	.62	34.90
1736.76	.32	36.31
1736.22	.02	37.73
1736.65	-.28	39.14
1735.44	-.58	40.55
1735.52	-.88	41.97
	Set II	
1735.28	1.57	28.44
1735.09	1.27	29.85
1735.52	.97	31.26
1735.81	.67	32.67
1735.35	.37	34.08
1736.20	.07	35.49
1736.09	-.23	36.91
	Set III	
1737.68	2.19	17.61
1736.08	1.89	19.02
1736.78	1.60	20.42
1735.74	1.30	21.83
1735.37	.99	23.24
1734.93	.69	24.64
1734.79	.39	26.05
1734.62	.08	27.47
	Set IV	
1737.74	1.69	6.38
1737.77	1.39	7.79
1738.62	1.09	9.19
1738.37	.78	10.60
1736.93	.47	12.01
1736.67	.15	13.48
1737.05	-.16	14.89
	Set V	
1736.90	1.68	-8.61
1737.17	1.35	-7.14
1737.00	1.04	-5.74
1736.76	.73	-4.33
1736.78	.42	-2.92
1736.77	.11	-1.51

Radii, km	Latitude, deg	Longitude, deg
	Set VI	
1737.25	-1.97	-10.96
1737.61	-2.27	-9.55
1737.69	-2.56	-8.15
1737.70	-2.86	-6.71
1737.51	-3.15	-5.29
1737.49	-3.44	-3.86
1738.33	-3.68	-2.68
1736.89	-4.01	-1.00
	Set VII	
1737.29	-1.64	-30.04
1737.20	-1.94	-28.62
1736.96	-2.23	-27.20
1736.97	-2.54	-25.72
1736.68	-2.83	-24.29
1736.76	-3.12	-22.86
1736.78	-3.41	-21.44
	Set VIII	
1736.15	-1.78	-43.24
1736.41	-2.07	-41.83
1736.25	-2.37	-40.41
1736.13	-2.66	-38.99
1735.75	-2.95	-37.56
1735.88	-3.23	-36.14
	Set IX(a)	
1735.76	-0.60	-50.89
1735.87	-.90	-49.48
1735.76	-1.19	-48.06
1735.72	-1.49	-46.65
1735.99	-1.78	-45.23
1735.60	-2.08	-43.81
1735.76	-2.37	-42.39
	Set IX(b)	
1735.97	-0.88	-51.54
1736.04	-1.18	-50.14
1735.66	-1.47	-48.72
1735.60	-1.77	-47.30
1735.85	-2.05	-45.88
1735.67	-2.35	-44.47
1735.74	-2.64	-43.06

TABLE II.- COMPARISON OF LUNAR ORBITER I VALUES OF LUNAR RADIUS WITH RADAR AND PHOTOGRAMMETRIC VALUES

Lunar Orbiter				Radar			
Latitude, deg	Longitude, deg	Radius, km	Accuracy, km	Latitude, deg	Longitude, deg	Radius, km	Accuracy, km
-2.86	-6.71	1737.70	±0.7	-2.95	-6.72	1737.17	±0.3
-3.15	-5.28	1737.50		-2.27	-5.96	1737.36	
1.05	-5.74	1737.00		1.17	-5.27	1737.21	
.73	-4.33	1736.76		.70	-4.51	1737.34	
Lunar Orbiter				Photogrammetric			
0.37	34.08	1735.35	±0.7	0.37	34.08	1734.82	±0.2
.07	35.49	1736.20		.07	35.49	1735.82	
-.23	36.91	1736.09		-.23	36.91	1735.60	
.11	-1.51	1736.77		.11	-1.51	1736.13	
-3.23	-36.14	1735.88		-3.23	-36.14	1735.31	
-2.08	-43.81	1735.60		-2.08	-43.81	1735.31	
-2.37	-42.39	1735.76		-2.37	-42.39	1735.26	
-2.35	-44.47	1735.67		-2.35	-44.47	1735.65	
-2.64	-43.06	1735.74		-2.64	-43.06	1735.42	

TABLE III.- ELLIPTICAL REPRESENTATION OF THE LUNAR EQUATOR

Ellipse	Set	Semimajor axis, km	Semiminor axis, km	Eccentricity	Mean radius, km
1	I, II	1736.66	1735.32	0.039360	1735.99
2	I, II, IV	1737.67	1733.29	.070989	1735.48
3	I, II, III, IV	1737.18	1733.62	.063929	1735.40
4	V, VI, VII, VIII, IXa, IXb	1737.31	1734.54	.056526	1735.92
5	III, V, VI, VII, VIII, IXa, IXb	1737.04	1734.59	.053076	1735.82
6	I, II, III, IV, V, VI, VII, VIII, IXa, IXb	1737.18	1734.38	.056794	1735.78

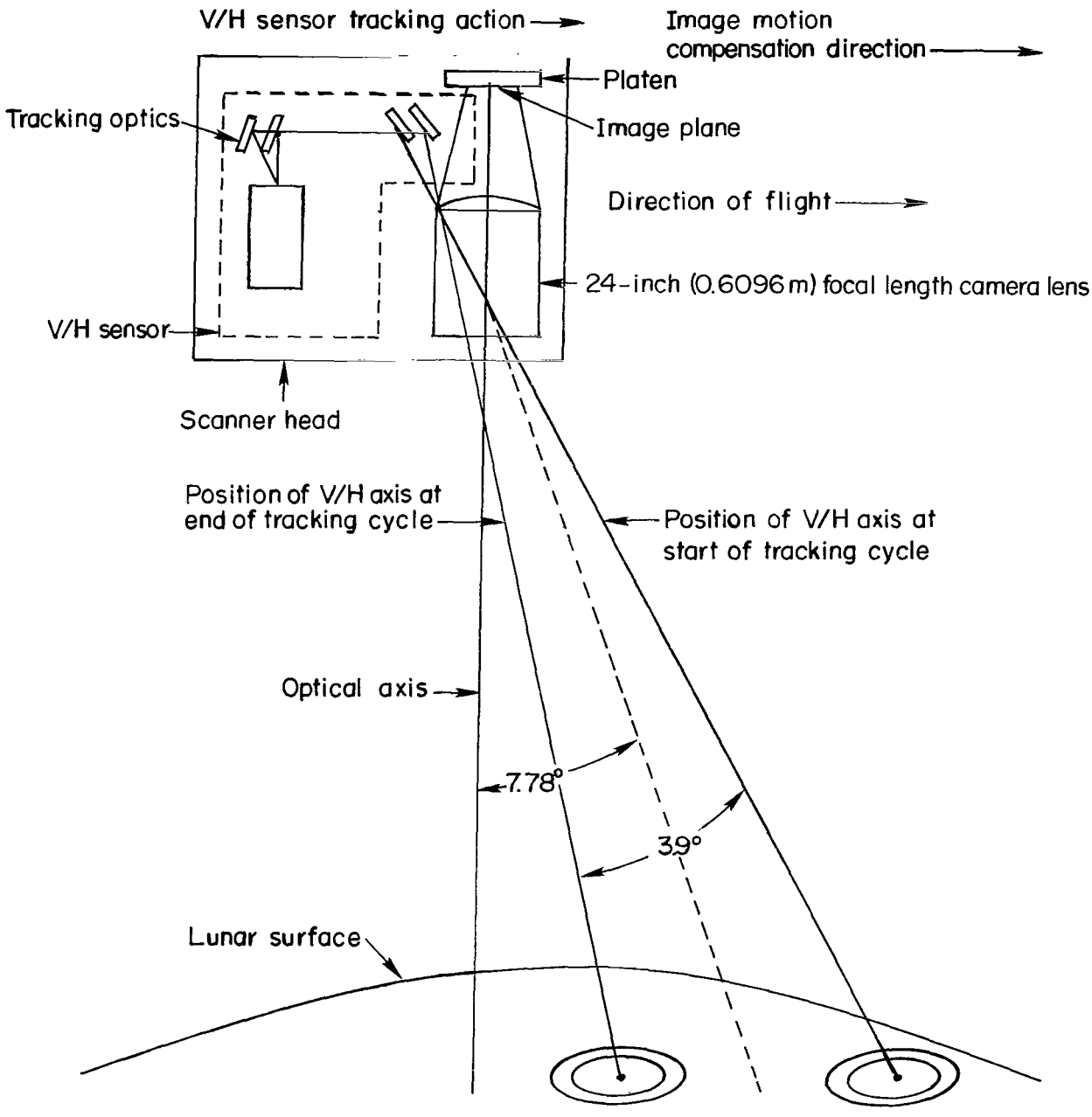

Figure 1.- Illustration of V/H sensor operation. (From ref. 1.)

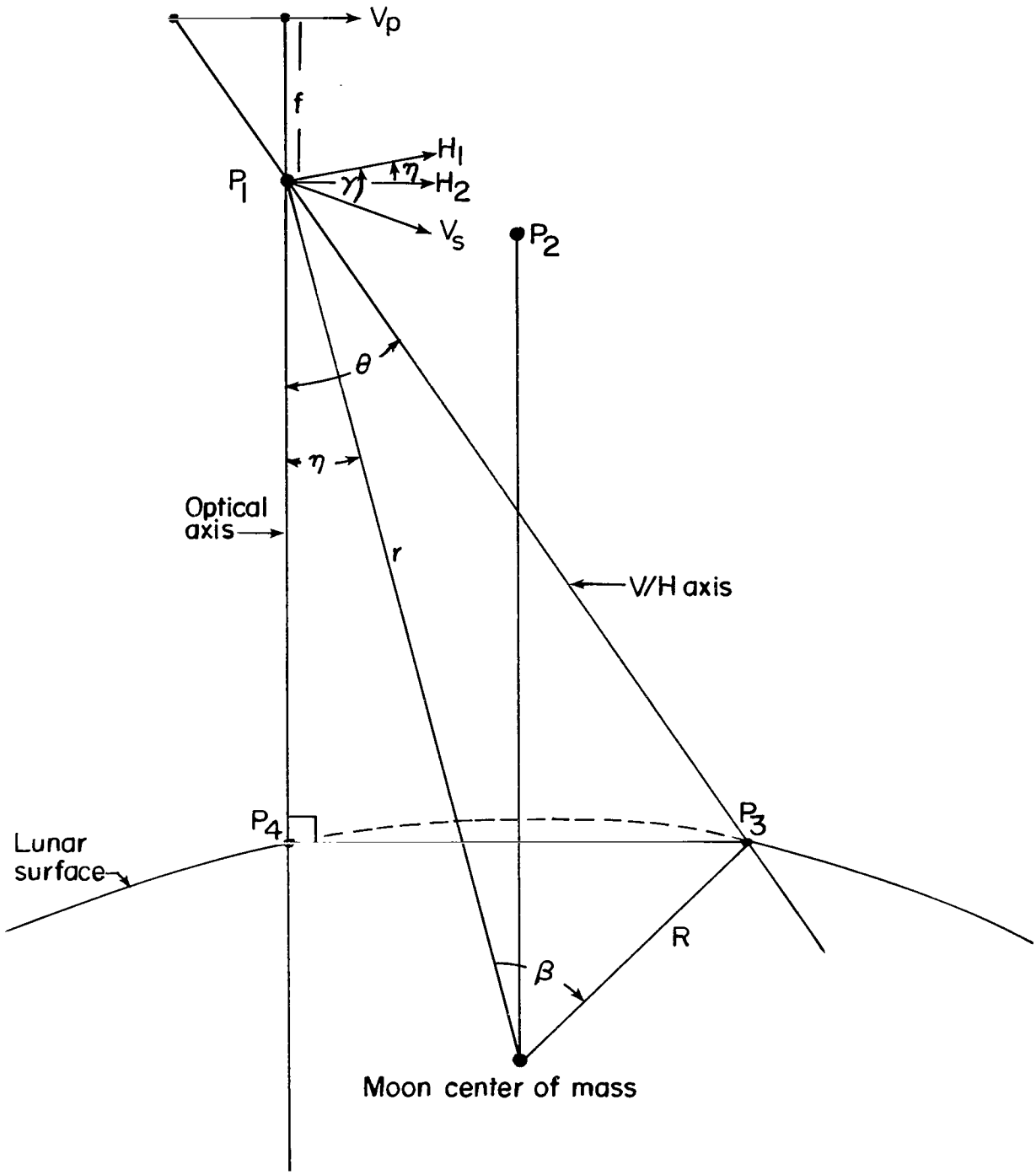

Figure 2.- Illustration of spacecraft—lunar-surface geometry.

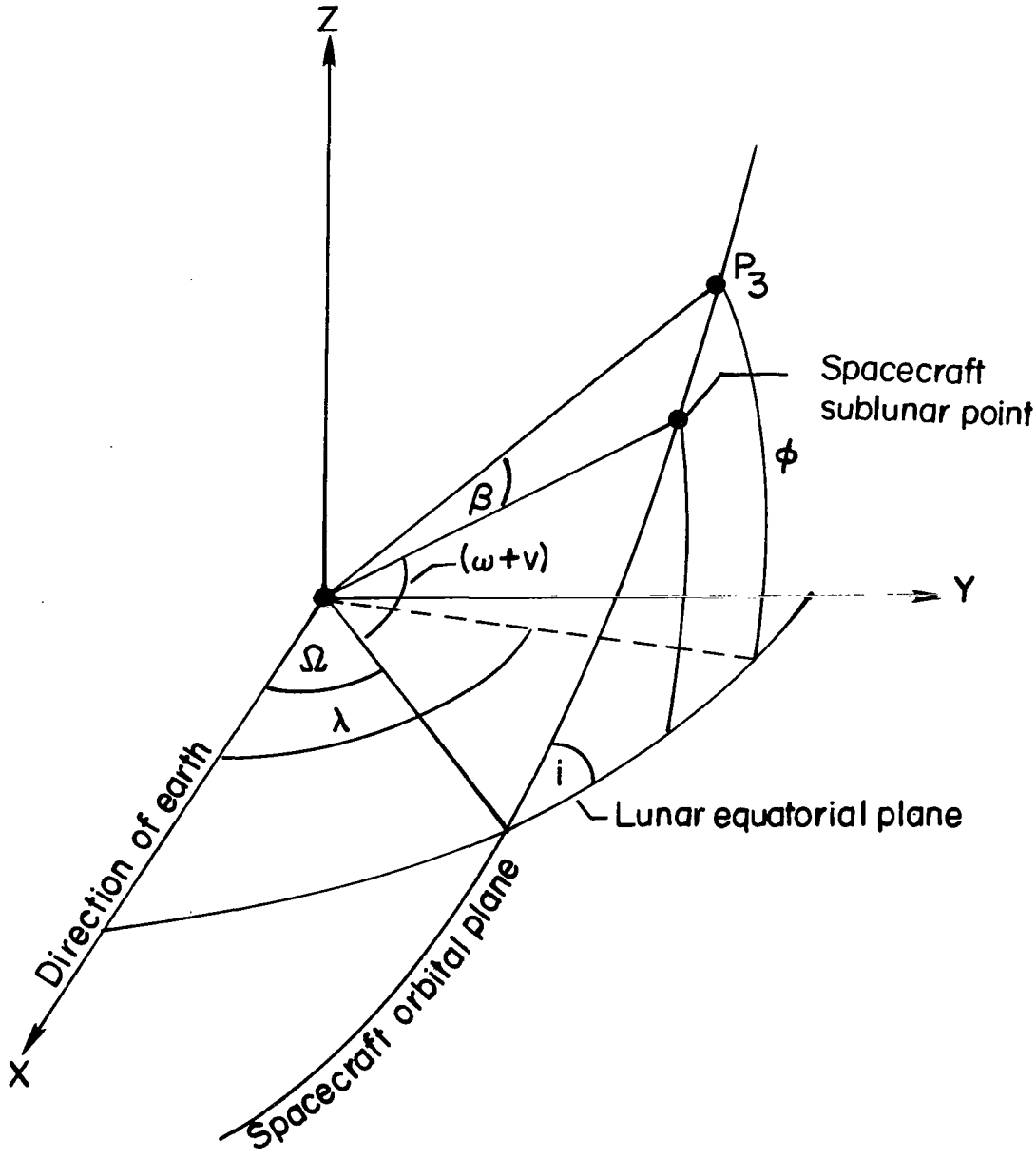

Figure 3.- Illustration of lunar satellite orbital parameters with respect to a selenographic coordinate system.

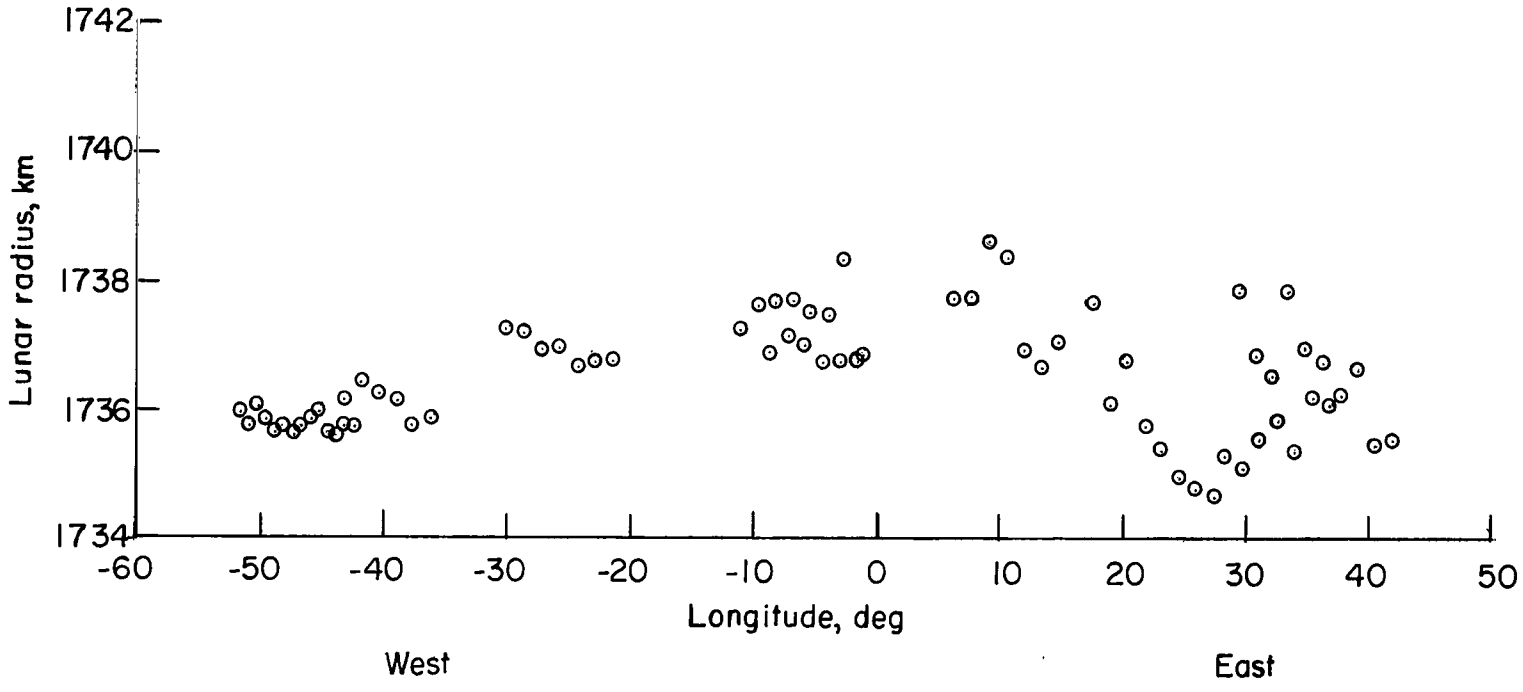

Figure 4.- Lunar equatorial radii determined from V/H sensor data on Lunar Orbiter I.

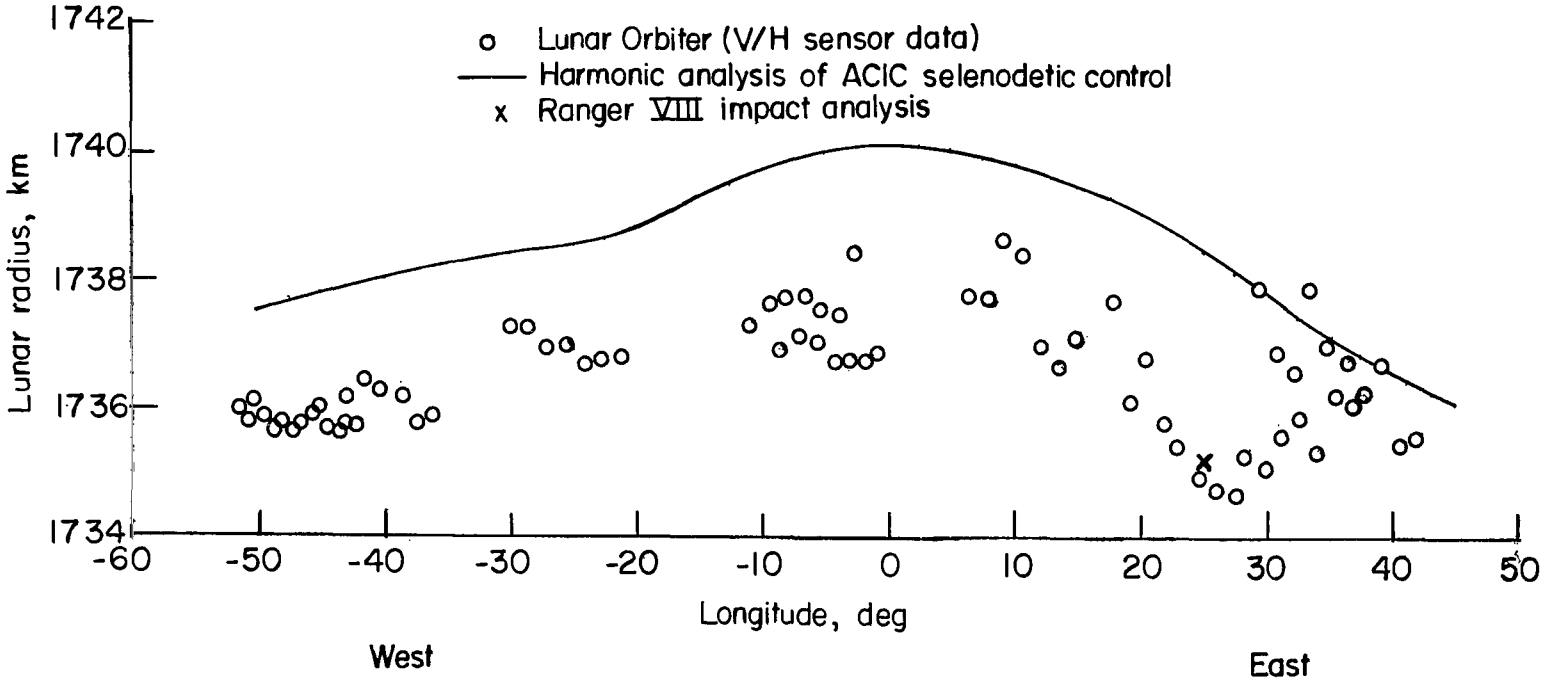

Figure 5.- Comparison of Lunar Orbiter I values of the lunar radius with those from a harmonic analysis and Ranger VIII input analysis.

NATIONAL AERONAUTICS AND SPACE ADMINISTRATION
WASHINGTON, D.C. 20546
OFFICIAL BUSINESS

FIRST CLASS MAIL

POSTAGE AND FEES PAID
NATIONAL AERONAUTICS AND
SPACE ADMINISTRATION

POSTMASTER: If Undeliverable (Section 158 Postal Manual) Do Not Return

"The aeronautical and space activities of the United States shall be conducted so as to contribute . . . to the expansion of human knowledge of phenomena in the atmosphere and space. The Administration shall provide for the widest practicable and appropriate dissemination of information concerning its activities and the results thereof."

—NATIONAL AERONAUTICS AND SPACE ACT OF 1958

NASA SCIENTIFIC AND TECHNICAL PUBLICATIONS

TECHNICAL REPORTS: Scientific and technical information considered important, complete, and a lasting contribution to existing knowledge.

TECHNICAL NOTES: Information less broad in scope but nevertheless of importance as a contribution to existing knowledge.

TECHNICAL MEMORANDUMS: Information receiving limited distribution because of preliminary data, security classification, or other reasons.

CONTRACTOR REPORTS: Scientific and technical information generated under a NASA contract or grant and considered an important contribution to existing knowledge.

TECHNICAL TRANSLATIONS: Information published in a foreign language considered to merit NASA distribution in English.

SPECIAL PUBLICATIONS: Information derived from or of value to NASA activities. Publications include conference proceedings, monographs, data compilations, handbooks, sourcebooks, and special bibliographies.

TECHNOLOGY UTILIZATION PUBLICATIONS: Information on technology used by NASA that may be of particular interest in commercial and other non-aerospace applications. Publications include Tech Briefs, Technology Utilization Reports and Notes, and Technology Surveys.

Details on the availability of these publications may be obtained from:

SCIENTIFIC AND TECHNICAL INFORMATION DIVISION

NATIONAL AERONAUTICS AND SPACE ADMINISTRATION

Washington, D.C. 20546